Influence of the oxide phase on the process of inflation of composition from highly dispersed porous iron

Influence of the oxide phase on the process of inflation of composition from highly dispersed porous iron

S Ya Alibekov[1], V A Dovydenkov[1], O S Zvereva[1], A V Egorov[1], A I Pavlov[1], A V Lysyannikov[2], Yu F Kaizer[2] and A I Demchenko[2]

[1] Volga State University of Technology, 3, Lenina Square, Yoshkar–Ola, 424000, Russia
[2] Siberian Federal University, 82/6, Svobodny ave., Krasnoyarsk, 660041, Russia

E–mail: kaiser171074@mail.ru

Abstract. The article describes a new technology for the production of steel parts for structural purposes. The technology is based on molding mixtures of iron powders, iron oxide powders and a binder. Technological processes include the processes of vacuum reduction of iron oxide and a binder material with subsequent sintering of the mixture. The study of the features of the brass infiltration process is carried out on highly porous iron-based blanks with pore sizes less than 1 μm with various percentages of the starting components. The analysis of the structures and mechanical properties of materials obtained on the basis of the developed technology has been performed. The mechanism of infiltration of highly iron-based preforms based on iron obtained by casting from the compositions "iron-iron oxide-phenol-formaldehyde resin" obtained in three stages is established. Recommendations have been developed for the pilot production of products of complex shape from iron-based metal powders, including of casting molding operations, oxide reduction and sintering operations, followed by brass infiltration and heat treatment of the products. The introduction of new technology makes it possible to produce products of complex shapes with a high level of mechanical properties, improved dimensional accuracy and lower cost.

1. Introduction

Pseudo-alloys based on iron and copper obtained by infiltration are increasingly used in industry, due to a combination of necessary performance characteristics that are not achievable in traditional materials[1-3], as well as high profitability of their use [4-9]. The volume of production of these products could have been significantly larger if there had been no restrictions on the configuration of products in existing technologies.

Traditional processes of pressing and sintering of iron powders with an average dispersion (30-150 microns) are usually used to obtain blanks based on iron with subsequent infiltration of it with copper alloys. Accordingly, the shape of the resulting products is subject to certain restrictions on the thickness of the walls, the ratio of thickness and height, the shape of the holes, etc. These restrictions can be avoided if new technologies of powder metallurgy are used in the production of billet, based on the processes of injection molding products of complex shapes from compositions consisting of thin powders (less than 30 micrometer) and a binder. However, highly dispersed iron powders for injection compositions, usually obtained by the carbonyl method, are significantly more expensive than medium-dispersed powders. It is known that metal and oxide powders can be molded by casting

methods. The use of oxides as components of injection molding compositions will significantly reduce the cost of raw materials. In addition to solving the problem of product shaping, this approach is promising from the point of view of forming highly dispersed structures in order to obtain materials with improved physical and mechanical properties.

2. Purpose of work

Study of the process of infiltration of porous powder materials by copper alloy of highly dispersed billet of complex shape, from iron powders and their oxides, with different percentages of the initial components and analysis of the obtained physical and mechanical properties of the material.

3. Tasks

1) Select a process mode of infiltration of porous powder materials; 2) Investigate the kinetics of the infiltration process of porous powder materials; 3) Investigate the influence of the oxide phase on the infiltration process and on the obtained physical and mechanical properties.

4. Analytical modeling

A second-order nonlinear differential equation is chosen to describe the infiltration process. It includes all significant resistance forces: inertia of the liquid in the reservoir (source of the liquid phase) and gas in the pores of the frame; viscous friction of gas and liquid in the pores of the frame, the weight of the liquid column. It also includes the driving force of the infiltration – capillary force, taking into account relaxation of the contact angle θ (t) from the value at the moment of contact of the porous frame with the liquid θ (0) = π / 2 up to an equilibrium value θp.

$$h_0 h'' + V_0 h' + \frac{hh'}{t_v} + gh = V_k^2\left(1 - e^{-t/\tau_\theta}\right), \tag{1}$$

$$h_0 = \frac{7Bd}{12} + \frac{\rho_{gas}}{\rho_{melt}} LB^2;$$

$$V_0 = \frac{32LB^2\eta_{gas}}{d^2\rho_{melt}};$$

$$t_V = \frac{d^2\rho_{melt}}{32LB^2\eta_{melt}};$$

$$V_k^2 = \frac{4\sigma_{melt}\cos\theta_e}{d\rho_{melt}} \tag{2}$$

where B is pore tortuosity coefficient; d- the pore diameter of the frame, *m*; ρ_{gas} is density of the protective gas atmosphere, *kg/m*^{3}; ρ_{melt} is the density of the melt, *kg/m*^{3}; L is height of the porous frame, *м*; η_{gas} is viscosity of the protective gas atmosphere, *Pa·s*; η_{melt} is melt viscosity, *Pa·s*; σ_{melt} is melt surface tension coefficient, *N/m*; θ_e is equilibrium wetting edge angle, *grad*; τ_θ is relaxation time of the wetting edge angle, *s*; *h, h′, h″* are height, speed, and acceleration of the melt front lift, *m, m/s, m/s*^{2}; *t* is time the infiltration, *s*.

Diffusion processes are active at the infiltration temperature, that cause mutual alloying of the steel frame and the copper melt, frame dissolution and liquid-phase rearrangement of frame particles, then, during the infiltration process, the pore size of the frame changes, as well as the density, surface tension coefficient, and viscosity of the melt.

Taking into account temporary changes in physical quantities $d = d(t)$, $p_{melt} = p_{melt}(t)$, $\sigma = \sigma_{melt}(t)$. $\eta_{melt} = \eta_{melt}(t)$ expression (2) they will have the following form:

$$h_0 = \frac{7Bd(t)}{12} + \frac{\rho_{gas}}{\rho_{melt}(t)} LB^2;$$
$$V_0(t) = \frac{32LB^2\eta_{gas}}{d^2\rho_{melt}};$$
$$t_V(t) = \frac{d^2(t)\rho_{melt}(t)}{32LB^2\eta_{melt}(t)};$$
$$V_k^2(t) = \frac{4\sigma_{melt}(t)\cos\theta_e}{d\rho_{melt}} \quad (3)$$

In the process of isothermal infiltration, the melt viscosity changes from a certain initial value $\eta_{melt}(0) = \eta_0 e^{Q/RT}$ equilibrium value $\eta_{melt}(\infty) = \eta_{melt}(0)\cdot(1+k_{melt})$, a change in the melt viscosity as a function of temperature, the solubility limit of iron in copper, as well as the concentration of various functional additives in the work [12] is proposed in the form of a relaxation equation

$$\eta_{\Xi}(t) = \eta_0 \exp\left(\frac{Q}{RT}\right)\cdot(1+k_v(1-\exp(-t/\tau_{melt}))) \quad (4)$$

where Q is the energy of activation, *Joule/mole*; η_0 is a multiplier, *Pa·s*; τ_{melt} is the relaxation time of melt viscosity, *s*; k_v is coefficient of increase in viscosity during infiltration.

Changing the pore size during infiltration due to liquid phase rearrangement from a certain initial value *d(0)* up to the equilibrium value $d(\infty) = d/(0)\cdot(1 - k_d)$ it was also taken into account by the relaxation equation

$$d(t) = \mathrm{d}/(0)\cdot(1 - k_d(1-\exp(-t/\tau_d))), \quad (5)$$

where τ_d is the relaxation time of the pore size of the frame, *m*; k_d is a reduction ratio of size of the pores in the infiltration process.

It can be assumed that the process of infiltration of frames with submicrocrystalline size will have its own characteristics, due to size factors. This applies to the kinetics of infiltration, the processes of interaction between the frame and the infiltrate, the requirements for technological modes, dimensional changes in the infiltrated products, their structure and physical and mechanical characteristics.

5. Experimental technique

The initial components for the manufacture of infiltrated samples were: iron powder A100S, iron powder (II, III) oxide ElectrOxide 20. Bulk density was determined according to GOST 19440-94. Phenol formaldehyde resin (FFS) (GOST 20907-75) was used as a binder.

Semi-finished products were made from these components by mixing the starting components, drying, granulation and crushing, followed by injection molding. The compositions were formed by direct press-casting into oblong block of 10x10x55 *mm* in size at a pressure of up to 20 *MPa* at temperatures from 120 to 130 ℃ with at 4 to 6 minutes. Next, the billet was subjected to heat treatment in order to remove the binder and the reduction of oxides. Heat treatment was performed in 3 stages: 1st stage: in a container with a fusible fuse; stage 2: in the forevacuum; and the 3rd stage samples were sintering in the endogas environment. Next, the samples were infiltrated with L63 grade brass at a temperature of 950 °*C* for 30 seconds. After each operation, the density, size, and structure were determined on the samples. Dimensional changes after infiltration were determined by direct measurements of the samples. The structure of the materials was studied on an EC METAM RV metallographic aggregate microscope, as well as on the INTERGA Prima probe microscope. In this work, we used contact scanning.

6. Interpretation of results

To study the infiltration process, several compositions differing in the content of components were used.

The main composition was chosen (vol. %): Fe (iron powderA100S) – 52.1 %; Fe_3O_4 (iron oxide powder (II, III) ElectrOxide 20) – 20.9 %; phenol formaldehyde resin – 27.0 %, the ratio of components ensures the forming of billet by the injection method with the maximum content of iron powder of average dispersion. To study the degree of influence of highly dispersed iron on the nature of the infiltration process, samples with a reduced content of average dispersion iron particles were made Fe – 40 vol. % и 30 vol. %).

Table 1 shows the initial composition and characteristics of samples of billet for infiltration, 10x10x55 *mm* in size. The compositions of the components were selected so that the volume fraction of the binder ensured fluidity during molding of the preforms, and the ratio of the mass fractions of phenol formaldehyde resin and oxides was sufficient to maintain the carbon balance during reduction.

Table 1. Composition and properties of the samples for infiltration.

No. composition	Initial composition, %	Density after sintering, kg/m^3	Porosity after sintering, %
1	Fe – 52.1 Fe_3O_4– 20.9 FFS – 27.0	5250	30.0
2	Fe - 40.2 Fe_3O_4 -26.2 FFS – 33.6	4690	31.0
3	Fe - 30.2 Fe_3O_4 -30.2 FFS – 39.6	4170	32.0

The structure of the billet for infiltration obtained from the main structure (figure 1a) consists of ferrite grains with sizes of 30-150 microns with small inclusions of perlite (about 10 %), around which sections with a fine grained and highly porous structure are distributed, consisting of approximately 80 % ferrite and 20 % perlite with a grain size of 3-5 microns.

Fine grained sections of the ferrite-perlite structure are iron reduced by FFS pyrolysis products. The pore size is from 0.1 to 3 microns (figure 1b).

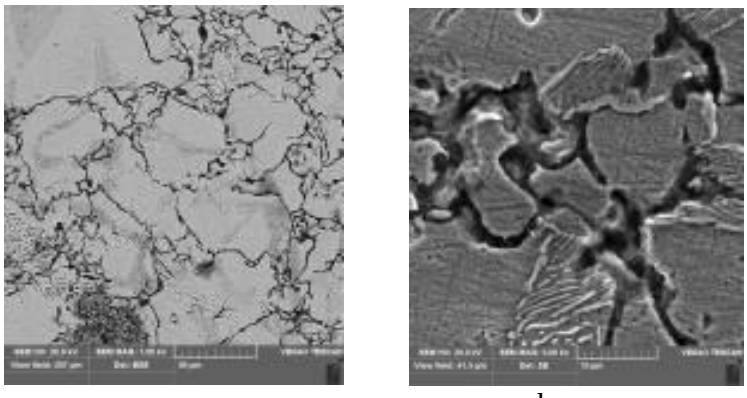

a b

Figure 1. Structure of the infiltration sample obtained on the scanning electron microscope: a – scan area 50x50 microns; b – scan area 5x5 microns.

According to the conduct research of the chemical composition of the material, no oxides iron and oxygen were found in the obtained billets. X-ray structural analysis showed that the material is single-phase with a volume-centered cubic lattice.

Thus one might argue that the carbon released as a result of thermal degradation has high reactivity and enters into chemical interaction with the original composition, actively and almost completely restoring the introduced iron oxide. An analysis of the chemical composition of the material according to the results of the X-ray fluorescence research method showed the following elements: Cu – 0.08%, Cr – 0.23%, Mn – 0.15 %, the rest – Fe.

As the material of the infiltrate, grade L63 brass was used, a two-component alloy with a single-phase structure α – a solid solution of zinc substitution in copper. The melting temperature of the brass is 906 ° C. From the Cu-Zn state diagram it follows that for this composition, at a temperature of 834 ° C, a liquid phase appears. This temperature is the beginning of the infiltration process, which was confirmed by the results of experiments. Next, studies were conducted on the infiltration of the developed materials at temperatures of 950 and 1000 °*C* with various isothermal holding times.

Figure 2 shows photographs of structures obtained using an optical microscope after infiltration at 950 °*C* with an isothermal holding of 15, 30, 60, 600 seconds.

The filling of pores ends within 15 seconds (figure 2a), while brass dissolves the highly dispersed iron located between the particles of iron of medium dispersion, as a result of which the areas filled with copper alloy increase. At the same time, processes of surface dissolution of iron particles of medium dispersion in copper occur — the boundaries of the iron particles are “blurred” (figure 2a, 2b). In addition, there is dissolution of copper in iron. In this case, the structure remains undissolved highly dispersed iron in the form of irregularly shaped particles and pieces with a size of 1÷8 microns (figure 2b) and their sizes increase with increasing holding time (figure 2c). During the subsequent cooling of the system, the iron-based phase precipitates from the supersaturated solution in the form of spherical particles with dimensions of 1÷5 microns (Figure 2d)

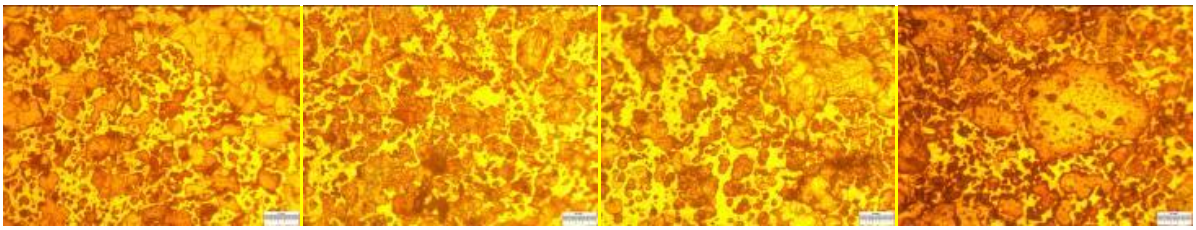

a b c d

Figure 2. Structure of samples after infiltration with different holding times: a – holding at 15 seconds at t = 950 °*C* x200, b – holding 30 seconds at t=950 °*C* x200, c – holding 60 seconds at t = 950 °*C* x200, d – holding a 600 seconds at t = 950 °*C* x200.

The microstructure of the samples after infiltration consists of areas of doped and supersaturated ferrite along the boundaries (30-150 micrometer), the space around which is filled with the copper phase and areas of doped ferrite (1-8 micrometer).

Analysis of the chemical composition of the material showed: Cu – 27.11 %, Zn – 11.72 %, Mn – 0.11 %, rest – Fe. As a result of X-ray diffraction analysis, two phases were found in the material: with a body-centered cubic lattice based on iron and with a face-centered cubic lattice based on copper.

The regularity obtained above required more in-depth studies regarding the kinetics and mechanism of the infiltration process and the materials under consideration. Figure 3 shows the experimental points of the dependence of the height of the front of the infiltrate on the holding time of the system at a given temperature. The height of penetration of the front of the copper alloy was determined using metallographic analysis on the thin micro-section as the distance from the end of the sample, where was the infiltrate to the extreme point of the boundary of the iron-copper system with an error of not

more than 0.2 mm. Infiltration was carried out at a temperature of 950 °*C* with a holding time of 3, 6, 9, 12, 15, 18 seconds. As experimental samples used samples of the compositions shown in table 1.

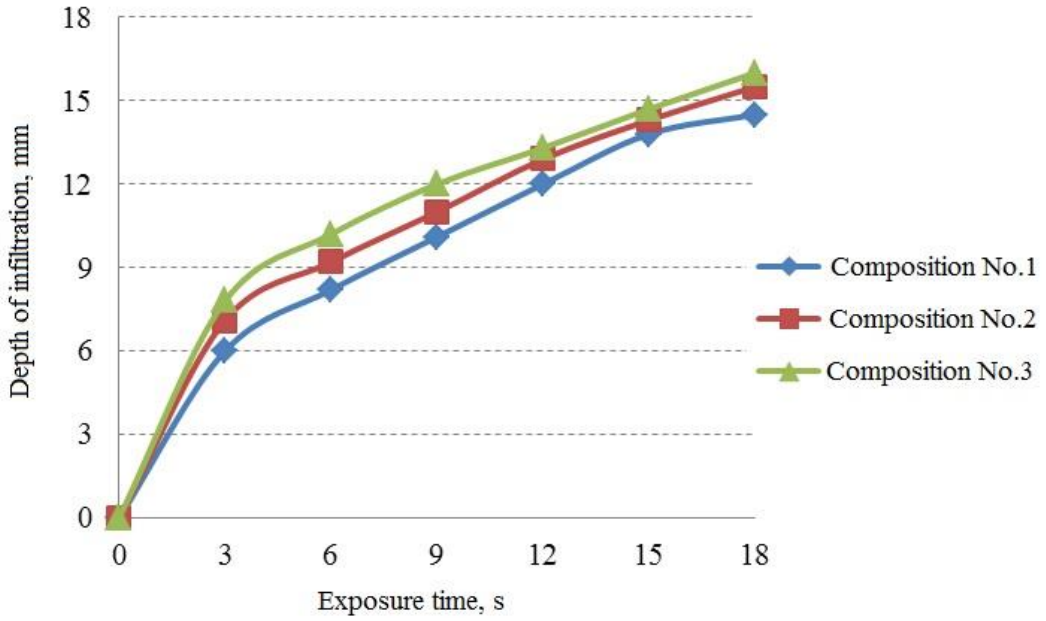

Figure 3. Experimental curves of penetration depth versus exposure time for materials of compositions No. 1, 2, 3.

From the graphs (Figure 3), it follows that the rate of the infiltration process depends on the composition and pore radius of the material. According to studies, the infiltration process is fairly accurately described by the Washburn equation, which is used for materials with pores of constant diameter:

$$l^2 = \frac{\sigma \cos \Theta r \tau}{2\eta}, \tag{6}$$

where σ is surface tension of the melt infiltrate, *millijoule/m*^{2}; Θ is the edge angle of wetting, °; r is pore radius, *m*; τ is duration of impregnation of the material with one of the compositions, *s*; η is kinematic viscosity of the melt infiltrate, *m*^{2}*/s*.

On the other hand, due to the difference between the surface energy of highly dispersed iron and the energy of the iron-infiltrate interphase boundary, a thermal effect occurs that contributes to a local increase in the.

The required level of physical and mechanical properties (Table 2) of iron-based composite powder infiltrated materials can be obtained by varying the parameters of the initial mixture composition quantitative content of the infiltrate material, temperature and time of isothermal holding, different methods of heat treatment.

Table 2. Density and hardness after infiltration at 950 ° C and holding time 60 seconds.

No. composition	Density after infiltration, *g/cm*^{3}	Hardness HB
1	7.85÷7.90	100±3
2	7.93±0.05	104±3
3	7.85÷7.90	112±3

7. Conclusion

1. The increase in the amount of the oxide phase in the mixture allows increasing the rate of the infiltration process and improve the hardness of the resulting material.

2. The use of iron oxide in the composition of the mixture allows obtaining parts of complex shape similar to Metal Injection Molding technology. The developed technology significantly expands the capabilities of powder metallurgy in the production of machine parts.

References

[1] Dovydenkov V A, Dovydenkova A V, Yarmolyk M V and Fetisov G P 2017 Optimization of the Component Compositions in a Composite Material Made of Mechanically Alloyed Cu-Al-O-C Granules and a Copper-Based Binder *Russian Metallurgy (Metally)* **13** 1109–11

[2] Dovydenkov V A and Zvereva O S 2014 Process of producing parts of complex shape by molding and sintering iron and iron oxide powders with a binder *Powder Metallurgy and Metal Ceramics* **52(9-10)** 594–9

[3] Morozov E A, Ablyaz T R, Muratov K R, Shlykov E S and Smolentsev E V 2020 Laser hardening of copper-iron pseudoalloy *Engineering Solid Mechanics* **8(2)** 83–92

[4] Gilev V G, Bezmaternykh N V and Morozov E A 2014 Study of steel–copper pseudo alloy microstructure and microhardness after laser heat treatment *Metal Science and Heat Treatment* **56(5–6)** 262–8

[5] Senillou H, Nouveau A and Lartigue J-F 2010 Development of a new generation of tungsten-copper composite powder for MIM *Proc. of the World Powder Metallurgy Congress and Exhibition, World PM* pp 4

[6] Kwon Y-S, Chung S-T, Lee S, Noh J-W, Park S-J and German R M 2007 Development of the high performance W-Cu electrode *Advances in Powder Metallurgy and Particulate Materials – 2007, Proc. of the 2007 Int. Conf. on Powder Metallurgy and Particulate Materials, PowderMet* pp 9111–8

[7] Huang Y, Yang K, Tang D and Chen W 2007 Study on strengthening of the solid contact alloy CuW80/Cu *Key Engineering Materials* **353–358(1)** 349–52

[8] Wildner H, Boening M and Pilz A 2008 Pseudo alloys of refractory and noble metals *Advances in Powder Metallurgy and Particulate Materials - 2008, Proc. of the 2008 World Congress on Powder Metallurgy and Particulate Materials, PowderMet* pp 938–44

[9] Lambjew D K and Todorow R P 1970 Study of sintered metal materials made of tungsten, molybdenum and silver powders *Electronics* [in Russian – Elektronika] **11(3)** 127–31